Surface Science 67 (1977) 77–88
© North-Holland Publishing Company

355

SURFACE RELAXATION ENERGIES IN CORE LEVEL SPECTROSCOPIES OF ADSORBED ATOMS AND MOLECULES

J.W. GADZUK
National Bureau of Standards, Washington, DC 20234, USA

Received 31 March 1977

Core level holes which are created in electron emission spectroscopies of atoms and molecules adsorbed or condensed onto metal surfaces induce a screening charge at the surface. The Coulomb interaction between the induced and the hole charge, called the extra-atomic relaxation energy, shifts the apparent binding energy of the ejected electron from the value inferred from an orbital energy. In this paper, linear response screening shifts are calculated for a number of different response functions which also allow for the polarizability of the adsorbed layers. The relation between classical image potential shifts and those obtained here is quantitatively compared. As an example, the X-ray photoelectron spectrum of SF_6 physisorbed on Ru surfaces is interpreted in terms of the present theory.

1. Introduction

Core level electron spectroscopy is a most fruitful endeavor for both elemental identification and chemical characterization of solid surfaces [1]. In general an incident beam of electrons or photons excites the solid in a way which ultimately leaves at least one hole in some core state and an electron in a high kinetic energy state. The electron can exit the surface and be energy analyzed. In addition, the surface can be left in an excited state due to the creation of phonons, electron-hole pairs, bulk plasmons, or surface plasmons. The ejected electrons emerge at discrete energies which are, to a first approximation, characteristic of the elemental nature of the source atom. However there are small (~1–10 eV) shifts in these characteristic energies which depend upon the immediate chemical environment of the source atom. Thus accurate determination of these shifts is quite useful in chemical analysis. As an example, the so-called electron binding energy (orbital energy with respect to a convenient zero, either the vacuum level or substrate Fermi level) of a core electron in an adsorbed molecule depends upon the separation between the molecule and the surface. Furthermore, the surface may dissociate the molecule, in which case yet another shift in the binding energy of the core electrons results. These "chemical shifts" arise from the differing electrostatic potentials at the core site in the various chemical situations (due to number and kind of and distance from nearest neighbors, degree of penetration through the surface dipole layer, etc.). The current status of chemical shifts and electron spectroscopy has been reviewed by Siegbahn [2].

Unfortunately this is not the complete story. The potential of the core hole polarizes the remaining electrons in the system. The Coulomb interaction between the polarization and the hole charge lowers the total energy of the ionized system. If the target system is left in the ground state of the new Hamiltonian which includes the core–hole potential, then the ejected electron must emerge with a greater kinetic energy than would be inferred from a "frozen electron" picture, in order that energy conservation holds. This upward shift is called the "relaxation energy." The ejected electron is observed at an energy which is displaced by both the chemical and relaxation shifts as shown in fig. 1 for an atom in the gas phase, on the surface, and embedded within the solid. To extract chemical shifts from observed spectra, one must know the relaxation shift.

A growing literature of relaxation theories exists, in which the emphasis is in either of two areas. First is the intra-atomic relaxation of all the electrons on the source atom, for which accurate calculational schemes are available [3]. If the

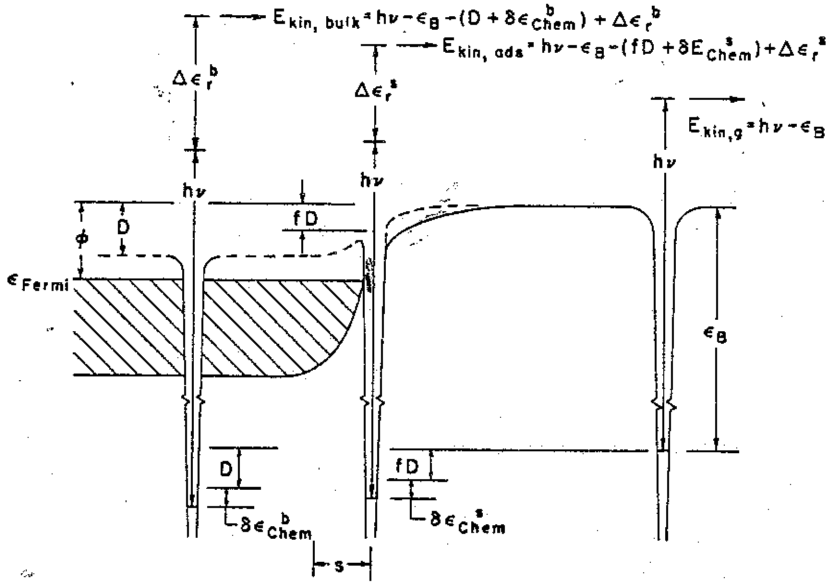

Fig. 1. Electrostatic-potential diagram relevant to photoejection of a core electron in a gaseous, adsorbed, and implanted atom, with respect to a surface of a metal with dipole potential D and work function ϕ. The kinetic energy of the ejected electron is given in terms of the photon energy $h\upsilon$, the gas phase binding energy ϵ_b, the fractional dipole penetration f, the remaining chemical shift δE_{chem}, and the extra-atomic relaxation energy $\Delta\epsilon_r$ which is the subject of this paper.

source atom is part of a molecule or solid, additional charge flow occurs to the hole. The resulting extra-atomic relaxation energy can be calculated in many different ways, each method having its own strengths and weaknesses [4–6].

It is usually assumed that the intra-atomic relaxation is identical in atoms and solids. If this is a good approximation, then in the condensed phase, the extra-atomic relaxation is just the energy associated with the screening of the hole. If the hole is located outside a surface, in the limit of large separations $\equiv s$ between the hole and the surface, the screening energy is just the classical image potential [7,8]. The purpose of this paper is to offer some new theory on image relaxation shifts. Since experimental electron emission spectra from adsorbed species are being analyzed in terms of image potential theories [9–13], it seems desirable to make these theories as realistic as possible. Hence the screening or image energy is calculated within a linear response formalism, for a number of different "reasonable" response functions. The semi-quantum mechanical step-density model for the surface has been adopted [14–16] in which the electron density of the solid is assumed to be uniform for $z \leqslant 0$. A charge sheet at $z = 0$ allows for the satisfying of boundary conditions on Maxwell's equations. This model is particularly useful for the type of parametric study presented here. This paper is intended to be a numerical complement to a previous work [7] in which more fundamental physics aspects of surface relaxation were stressed.

2. Theory

The magnitude of the extra-atomic relaxation energy is determined by the adiabatic Coulomb interaction between the adsorbate hole charge density $\rho_0(r; s)$ and the induced screening charge $\rho_{\text{in}}(r'; s)$,

$$\Delta\epsilon_s = \tfrac{1}{2}\int \mathrm{d}^3r\,\mathrm{d}^3r'\,\rho_{\text{in}}(r'; s)\,\frac{e^2}{|r - r'|}\,\rho_0(r; s)\,, \qquad (1)$$

where s is hole–surface separation and $z = 0$ defines the "surface" plane. Since core holes typically have radii $\lesssim 0.1$ Å, ρ_0 may be regarded as a point charge with $\rho_0(r; s) = \delta(z - s)\,\delta^{(2)}(r_\parallel)$. The role of hole spatial extent and shape has previously been investigated [7] with the general conclusion that $\Delta\epsilon_s$ decreases with increasing hole volume, although this decrease is inconsequential for core holes.

Introducing two-dimensional Fourier transforms parallel to the surface, eq. (1) can then be reduced to the convenient form [7,8,18]

$$\Delta\epsilon_s = \tfrac{1}{2}\int \frac{\mathrm{d}^2q_\parallel}{(2\pi)^2}\,v(q_\parallel)\,R(q_\parallel, 0)\,F(q_\parallel, s)\,, \qquad (2)$$

where the static linear response function

$R(q_{\|}, 0) = \delta\rho_{\text{in}}(q_{\|}, \omega = 0)/\delta\rho_0(q_{\|}, \omega = 0)$

relates the induced charge to the driving charge, $v(q_{\|}) = 2\pi e^2/q_{\|}$, and

$$F(q_{\|}, s) = \left|\int_{-\infty}^{\infty} \mathrm{d}z \exp(-q_{\|}|z|)\, \rho_0(q_{\|}, z)\right|^2 . \tag{3}$$

For the point holes considered here,

$\rho_0(q_{\|}; z) = \int \mathrm{d}^2 r_{\|} \exp(\mathrm{i}q_{\|} \cdot r)\, \rho_0(r) = \delta(z - s)$,

so $F(q_{\|}, s) = \exp(-2q_{\|}s)$. The quantum mechanical generalization of the image charge response function requires

$$R(q_{\|}, \omega) = [1 - \epsilon(q_{\|}, \omega)]/[1 + \epsilon(q_{\|}, \omega)] , \tag{4}$$

where $\epsilon(q_{\|}, \omega)$ is an appropriate dielectric function, to be discussed shortly. Combining eqs. (2)–(4) one obtains the well-known expression

$$\Delta\epsilon_s = \frac{e^2}{2} \int_0^{\infty} \mathrm{d}q_{\|} \left(\frac{1 - \epsilon(q_{\|}, 0)}{1 + \epsilon(q_{\|}, 0)}\right) \exp(-2q_{\|}s) . \tag{5}$$

A major point in eq. (5) is the exponential cutoff of the integrand for $q_{\|} \gtrsim 1/s$. Consequently only the small $q_{\|}$ components of the response function, eq. (4), are of importance. We now move on to specific model dielectric functions.

2.1. *Bulk response function*

The obvious first approximation is to evaluate the response function, eq. (4), using expressions for the homogeneous bulk dielectric function [7]. In the Fermi–Thomas approximation $\epsilon(q, 0) = 1 + \kappa^2/q^2$ with $\kappa = 2.95/r_s^{1/2}$ Å^{-1}.

The consequent response function is

$$R^{\mathrm{B}}_{\mathrm{FT}}(q) = 1/(1 + 2q^2/\kappa^2) . \tag{6}$$

Using eq. (6), the screening energy is given in terms of standard sine and cosine integrals as

$$\Delta\epsilon_s = \frac{e^2\kappa}{2\sqrt{2}} [\mathrm{ci}(\sqrt{2}\kappa s) \sin(\sqrt{2}\kappa s) - \mathrm{si}(\sqrt{2}\kappa s) \cos(\sqrt{2}\kappa s)] . \tag{7}$$

With the definition $y \equiv \sqrt{2}\kappa s$, the ratio of $\Delta\epsilon_s$ to the classical image potential = $e^2/4s$, is

$R(y) = y\,[\mathrm{ci}(y) \sin y - \mathrm{si}(y) \cos y]$

which is given in table 1.

This exercise can be repeated with a better dielectric function, such as the RPA

Table 1

Ratios of eq. (7) screening energy to classical image potential as a function of $y = \sqrt{2}\kappa s$

y	$R(y)$	y	$R(y)$
0.0	0.00	3.0	0.88
0.5	0.43	3.5	0.90
1.0	0.62	4.0	0.92
1.5	0.73	4.5	0.93
2.0	0.80	5.0	0.93
2.5	0.84		

where

$$\epsilon_{\mathrm{RPA}}(q,0) = 1 + \frac{0.165 r_{\mathrm{s}}}{x^2}\, u_{\mathrm{RPA}}(x)$$

with

$$u_{\mathrm{RPA}}(x) = \tfrac{1}{2}\left(1 + \frac{(1-x^2)}{2x}\ln\left|\frac{1+x}{1-x}\right|\right)$$

and $x = q/2k_{\mathrm{F}} = qr_{\mathrm{s}}/7.254$. Of course eq. (5) must then be integrated numerically.

Some useful insight into "allowable" surface approximations can be gained from fig. 2 in which various response functions versus q are plotted. Consider only the curves labeled $\epsilon_{\mathrm{B}}^{-1}$ and $R_{\mathrm{B}}(q_\parallel, 0)$ as a function of $q_\parallel$. The solid curves are RPA values whereas the dashed are Fermi–Thomas. For bulk screening, the Fermi–Thomas approximation always gives much too large screening charge density at the impu-

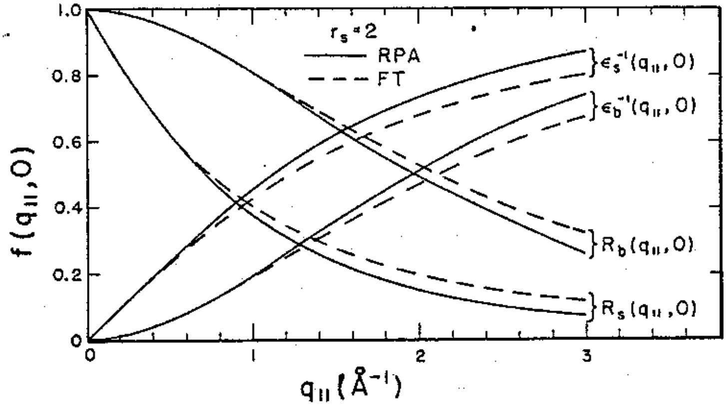

Fig. 2. An example ($r_{\mathrm{s}} = 2$) of some inverse dielectric ($\epsilon^{-1}(q_\parallel, 0)$) and response ($R(q_\parallel, 0)$) functions in the static limit, as a function of $q_\parallel$. RPA expressions are given by the full lines and Fermi–Thomas by the dashed lines.

rity site due to the breakdown of the approximation in the short wavelength (large q) region. In fig. 2, discrepancies between RPA and FT functions are insignificant for $q_\parallel < 1$ Å^{-1}. Now from eq. (5), the heavily weighted response occurs for $q_\parallel \lesssim 1/2s$ which is $\lesssim 0.5$ Å^{-1} for reasonable adsorbates. Consequently, the Fermi–Thomas response function is quite adequate in surface screening energy calculations, given the validity of a linear response theory in the first place.

2.2. Surface response function

A number of years ago, Ritchie and Marusak [14] presented a dielectric surface model in which the response of the solid to an exterior charge distribution was simulated by an infinitesimally thin charge sheet at the surface. This model, which presumes a uniform electron density in the solid up to $z = 0$ has been called the step density model. The limits of validity and usefulness of this model have also been critically discussed [14–17]. In essence Maxwell's equations are solved throughout space and the charge density sheet allows the matching boundary conditions of the interface to be satisfied provided the two-dimensional "surface dielectric function" of the electron gas–vacuum interface is related to the three-dimensional dielectric function of the homogeneous system through [14–18]

$$\epsilon_s(q_\parallel, \omega) = \left[\frac{q_\parallel}{\pi} \int_{-\infty}^{\infty} \frac{dq_z}{q^2 \epsilon(q, \omega)}\right]^{-1}, \tag{8}$$

with $q = (q_z^2 + q_\parallel^2)^{1/2}$. In the case of the static Fermi–Thomas limit, eq. (8) integrates to $\epsilon_s^{FT}(q_\parallel, 0) = (1 + \kappa^2/q_\parallel^2)^{1/2}$ and the response function is

$$R^s_{FT}(q_\parallel, 0) = (q_\parallel - (q_\parallel^2 + \kappa^2)^{1/2})^2/\kappa^2\,, \tag{9}$$

which is also plotted, for $r_s = 2$, in fig. 2. Note that in the $q_\parallel \to 0$ limit, R^s decreases linearly with increasing $q_\parallel$ whereas R^B is constant.

A closed form expression for the screening energy in the Fermi–Thomas surface dielectric approximation, which follows from eqs. (4), (5) and (9) is [19]

$$\Delta\epsilon_s = \frac{e^2}{4s}\{1 + 1/(\kappa^2 s^2) - 2S_{0,2}(2\kappa s)\}\,, \tag{10}$$

where $S_{0,2}$ is an in-principle-tabulated Lommel function whose first few expansion terms are $S_{0,2}(Z) = 1/Z + 3/2Z^2 + \ldots$. A standard approximate surface screening energy expression has been the displaced image plane expression $\Delta\epsilon_s \sim e^2/4(s + \kappa^{-1})$ first suggested by Gomer and Swanson [21]. Eq. (10) can be brought to the form $\Delta\epsilon_s \simeq e^2/4(s + \kappa^{-1}) + 0(1/s^2)$ which is similar.

2.3. Metal-dielectric surface response

In actual fact, the hole created in an adsorbed atom or molecule does not polarize the surface in the same way as does the point charge shown in fig. 3a. For a

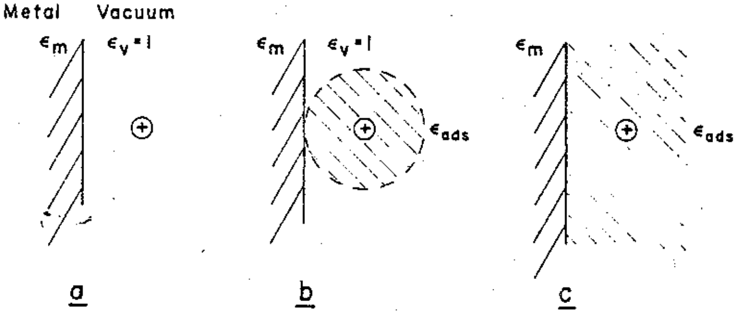

Fig. 3. Some idealized surface screening models. (a) Hole localized in a vacuum ($\epsilon_v = 1$) half space outside a metal characterized by a dielectric function ϵ_m. (b) Hole localized in a polarizable molecule outside a metal with ϵ_m. (c) Hole localized in a polarizable half space characterized by a dielectric constant appropriate to the particular molecule. The value of the screening energy of (b) should be bounded by the calculable values of (a) and (c).

single adparticle, as in fig. 3b, the hole polarizes the atom or molecule and the field which the surface responds to is due to the combined hole plus intra-molecular polarization charge. In the limit of a thick condensed layer, the hole can be imagined to be embedded in the dielectric continuum shown in fig. 3c. The surface dielectric function for the metal–dielectric interface, within the Ritchie–Marusak model, can readily be shown to be

$$\epsilon_{\rm tot}(q, \omega) = \left[\frac{q\epsilon_{\rm ads}}{\pi} \int_{-\infty}^{\infty} \frac{\mathrm{d}q_z}{q^2 \epsilon(q, \omega)}\right]^{-1}, \tag{11}$$

where $\epsilon_{\rm ads}$ is the dielectric constant of the adsorbed thick film. Combining eqs. (4) and (11), and rearranging, the surface response function for the configuration shown in fig. 3c is

$$R_{\rm s}(q_\parallel, \omega) = \frac{\epsilon_{\rm ads} - \epsilon_s(q_\parallel, \omega)}{\epsilon_{\rm ads} + \epsilon_s(q_\parallel, \omega)}, \tag{12}$$

where $\epsilon_s(q_\parallel, \omega)$ is given by eq. (8). Eq. (12) is just what would be guessed from the classical image potential arguments.

The complete expression for the screening energy of the hole embedded in a dielectric continuum matched to a metal is,

$$\Delta\epsilon_{\rm s} = \frac{e^2}{2\epsilon_{\rm ads}} \int_0^{\infty} \mathrm{d}q_\parallel \left(\frac{\epsilon_{\rm ads} - \epsilon_s(q_\parallel, 0)}{\epsilon_{\rm ads} + \epsilon_s(q_\parallel, 0)}\right) \exp(-2q_\parallel s) . \tag{13}$$

The ratio of $\Delta\epsilon_{\rm s}$ to the classical image energy $\epsilon_{\rm im} = e^2/4\epsilon_{\rm ads}s$ has been calculated, as a function of separation s, varying $\epsilon_{\rm ads}$ parametrically for a given value of r_s. The results are shown in figs. 4–7. The numbers displayed here were obtained from

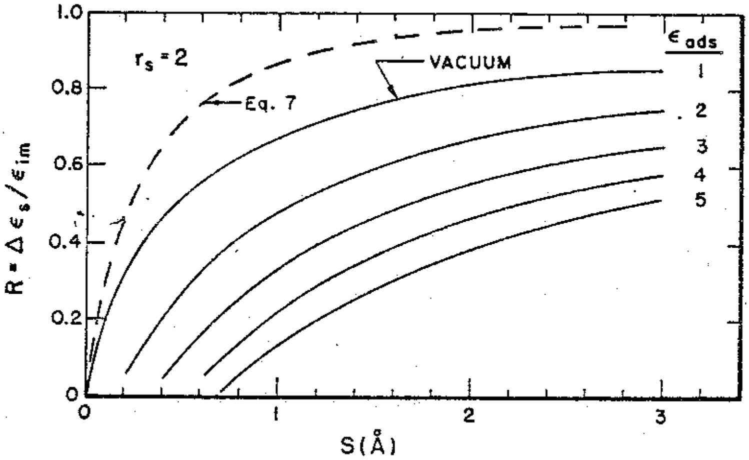

Fig. 4. Ratio of the surface screening energy given by eq. (13) to the classical image potential $\epsilon_{im} = e^2/4\epsilon_{ads}s$ as a function of the hole-screening plane separation treating ϵ_{ads} parametrically. Here $r_s = 2$.

Fermi–Thomas dielectric functions since a few trial calculations within the RPA produced results that were virtually indistinguishable from FT. As an example, eq. (7), the ratio obtained with the bulk response function, is also shown in fig. 4. Note the significant decrease in screening efficiency by the surface dielectric function at small separations.

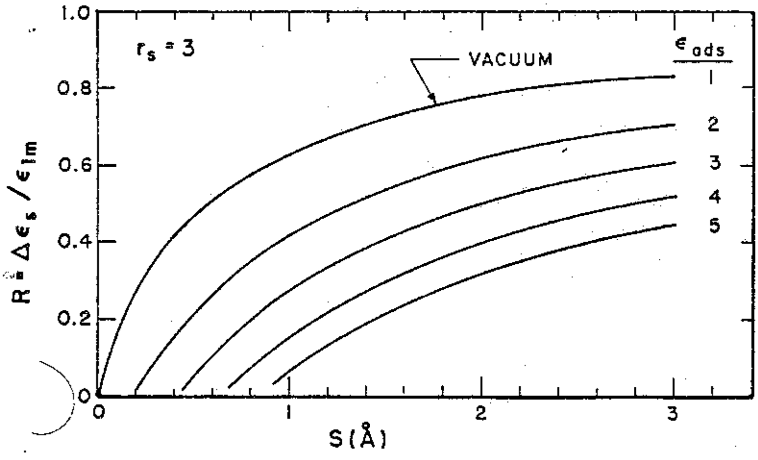

Fig. 5. Same as fig. 4 but with $r_s = 3$.

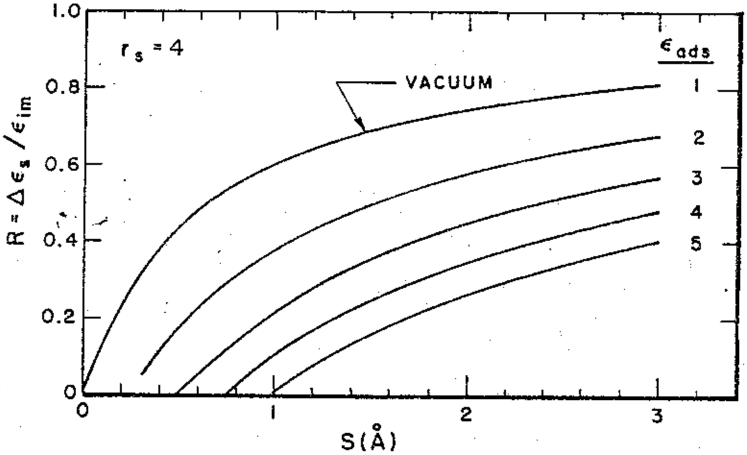

Fig. 6. Same as fig. 4 but with $r_s = 4$.

The reduction in the screening energy due to polarizability of the dielectric medium is a nontrivial effect for atomic scale hole–surface separations. It seems reasonable to expect that the true surface screening energy for a hole produced in an adsorbed polarizable layer is bounded by the vacuum ($\epsilon_{ads} = 1$)–metal value from above and the dielectric–metal value from below where the value of ϵ_{ads} is taken to be that for a pure solid of the adsorbed material. This exercise is the first one (to this writer's knowledge) in which some coupling between intra-adsorbed layer relaxation and metal screening have been considered, albeit in a very approximate way.

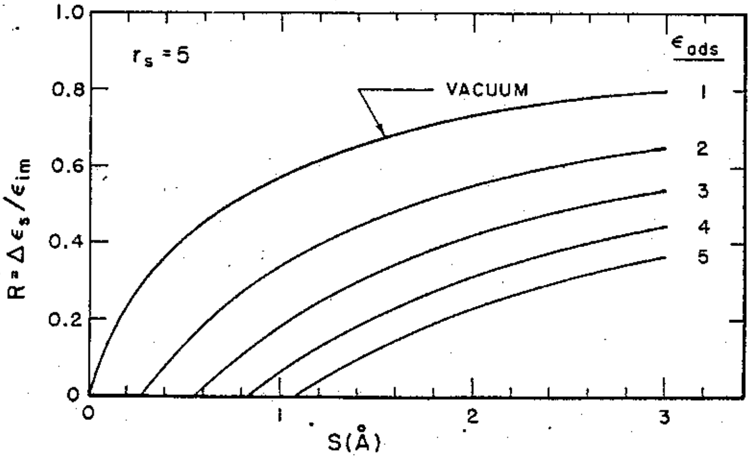

Fig. 7. Same as fig. 4 but with $r_s = 5$.

3. SF_6: an example

An interesting application of the image screening notions has been presented by Fisher et al. [13] in an X-ray photoemission study of SF_6 which had been physisorbed and condensed into a Ru(001) substrate. Here some refinements to their arguments are given, based on the ideas of this paper. The curious observation of Fisher and co-workers was an enhanced broadening of the F(1s) linewidth (1.75 ± 0.1 eV) for a monolayer of physisorbed SF_6, in contrast to a 1.35 ± 0.1 eV linewidth for either condensed or gas phase SF_6.

They felt that the most feasible interpretation of this effect was a differential relaxation shift amongst the various F atoms. The octahedral SF_6 is envisioned to adsorb in a configuration in which one plane of three F atoms is a distance s_1 from the surface and the plane containing the remaining three F atoms is a distance s_2 from the surface where it is known from the structure of SF_6 that $s_2 = s_1 + 1.91$ Å. The hypothesis is that the F(1s) hole suffers (or enjoys) a different screening shift depending upon which plane it is in and the 1.75 eV line is in fact an unresolved doublet. The data suggests a splitting of 0.7 ± 0.1 eV. From crystallographic considerations, Fisher assigned a value of $s_1 = 0.95$ Å and thus $s_2 = 2.86$ Å. For an $r_s = 2$ substrate and a vacuum halfspace ($\epsilon_{\text{ads}} = 1$), eq. (13) and fig. 4 yield $\Delta\epsilon_s(s_1) = 2.46$ eV and $\Delta\epsilon_s(s_2) = 1.07$ eV so the maximum doublet splitting is 1.39 eV. Considering the polarizable nature of SF_6 by letting $\epsilon_{\text{ads}} \sim 2$, fig. 4 yields $\Delta\epsilon_s(s_1) \simeq 0.85$ eV and $\Delta\epsilon_s(s_2) = 0.45$ eV so the minimum doublet splitting is ~0.4 eV. The observations fall right in the middle of the allowed range which is encouraging. Furthermore, these numbers were obtained by a straightforward implementation of the procedures suggested in ref. [7] and the present text. No fudging or readjustment of "input parameters" was required in order to get to a satisfactory end result. It is this sort of application for which the simple quantum image theories can be both useful and fundamentally correct.

4. Summary

The surface relaxation energy associated with core hole creation in an adsorbed atom or molecule has been calculated within a linear response dielectric screening model. Some modifications to the usual image screening energy, due to the polarizable nature of the adsorbed layer, have been included. Various dielectric response functions have been considered and it has been demonstrated why a simple Thomas response function is reasonable for surface screening. Finally, numerical values for screening energies vs. separation, treating both the substrate electron density and the adlayer dielectric constant parametrically, have been provided. Hopefully these will be of use in the quantitative analysis of spectroscopic surface data.

Acknowledgements

This study was aided by the healthy skepticism of Bill Unertl and discussion with Galen Fisher.

References

[1] Good entries into the (too) rapidly growing literature can be made through the survey articles in:
(a) Electronic Structure and Reactivity of Metal Surfaces, NATO A.S.I., Eds. E. Derouanne and A.A. Lucas (Plenum, New York, 1976).
(b) Treatise on Solid State Chemistry, Vols. 6A and 6B, Ed. N.B. Hannay (Plenum, New York, 1976).
(c) Experimental Methods in Catalysis, Vol. II, Eds. R.B. Anderson and D.T. Dawson (Academic Press, New York, 1976).
(d) Photoemission from Surfaces, Eds. B. Feuerbacher, B. Fitton and R. Willis (Wiley, New York, 1977).

[2] K. Siegbahn, Electron Spectroscopy for Solids, Surfaces, Liquids, and Free Molecules (to be published).

[3] D.W. Davis and D.A. Shirley, J. Electron Spectros. 3 (1974) 137; D.A. Shirley, R.A. Pollak, L. Ley, S. Kowalczyk and F.R. McFeely, Solid State Phys. (to be published).

[4] (a) Response screening theories:
B. Lundqvist, Physik Kondens. Mater. 6 (1967) 206;
L. Hedin and A. Johansson, J. Phys. B2 (1969) 1336;
D.C. Langreth, Phys. Rev. B1 (1970) 471;
D.C. Langreth, in: Collective Properties of Physical Systems, Eds. B. Lundqvist and S. Lundqvist (Academic Press, New York, 1974);
J.W. Gadzuk, Chem. Phys. Letters 36 (1975) 606.
(b) Additional response theories:
S.C. Ying, J.R. Smith and W. Kohn, Phys. Rev. B11 (1975) 1483;
L.M. Kahn and S.C. Ying, Surface Sci. 59 (1976) 333.

[5] P.M. Citrin and D.R. Hamann, Phys. Rev. B10 (1974) 4948;
R.E. Watson, J.F. Herbst and J.W. Wilkins, Phys. Rev. B14 (1976) 18;
R. Hoogewijs, L. Fiermans and J. Vennik, Chem. Phys. Letters 38 (1976) 471.

[6] R.V. Kasowski, Phys. Rev. Letters 37 (1976) 219;
P.S. Bagus and K. Hermann, Solid State Commun. 20 (1976) 5.

[7] J.W. Gadzuk, Phys. Rev. B14 (1976) 2267.

[8] A.C. Hewson and D.M. Newns, Japan. J. Appl. Phys. Suppl. 2, Part 2 (1974) 121;
B. Gumhalter and D.M. Newns, Phys. Letters 53A (1975) 137;
A. Datta and D.M. Newns, Phys. Letters 59A (1976) 326.

[9] J.T. Yates, Jr., N.E. Erickson, S.D. Worley and T.E. Madey, in: The Physical Basis for Heterogeneous Catalysis, Eds. E. Drauglis and R.I. Jaffee (Plenum, New York, 1975).

[10] J.C. Fuggle, E. Unbach and D. Menzel, Solid State Commun. 20 (1976) 89; D. Menzel in ref. [1d].

[11] W.D. Robertson, J. Vacuum Sci. Technol. (to be published).

[12] R. Brundle in ref. [1a].

[13] G.B. Fisher, N.E. Erickson, T.E. Madey and J.T. Yates, Jr., Surface Sci. 65 (1977) 210.

[14] R.H. Ritchie and A.L. Marusak, Surface 4 (1966) 234.

[15] R. Fuchs and K.L. Kliewer, Phys. Rev. B3 (1971) 2270.

[16] J. Heinrichs, Phys. Rev. B8 (1973) 1346.
[17] J. Harris, J. Phys. C5 (1972) 1757;
J. Harris and R.O. Jones, J. Phys. C6 (1973) 3585.
[18] J.W. Gadzuk, in ref. [1d].
[19] S. Gradshteyn and I.M. Ryzhik, Tables of Integrals, Series, and Products (Academic Press, New York, 1965) p. 985.
[20] R. Gomer and L.W. Swanson, J. Chem. Phys. 38 (1963) 1613;
D.M. Newns, J. Chem. Phys. 50 (1969) 4572.